Swarm Intell (2010) 4: 301–318
DOI 10.1007/s11721-010-0048-2

# Scale invariance of immune system response rates and times: perspectives on immune system architecture and implications for artificial immune systems

**Soumya Banerjee · Melanie Moses**

Received: 14 October 2009 / Accepted: 20 September 2010 / Published online: 23 October 2010


**Abstract** Most biological rates and times decrease systematically with increasing organism body size. We use an ordinary differential equation (ODE) model of West Nile Virus in birds to show that pathogen replication rates decline with host body size, but natural immune system (NIS) response rates do not change systematically with body size. The scale-invariant detection and response of the NIS is surprising since the NIS has to search for small quantities of pathogens through larger physical spaces in larger organisms, and also respond by producing larger absolute quantities of antibody in larger organisms. We hypothesize that the NIS has evolved an architecture to efficiently neutralize pathogens. We investigate three different hypothesized NIS architectures using an Agent Based Model (ABM). We find that a sub-modular NIS architecture, in which lymph node number and size both increase sublinearly with body size, efficiently balances the tradeoff between local pathogen detection and global response. This leads to nearly scale-invariant detection and response consistent with experimental data. Similar to the NIS, physical space and resources are also important constraints on distributed systems, for example low-powered robots connected by short-range wireless communication. We show that the sub-modular design principles of the NIS can be applied to problems such as distributed robot control to efficiently balance the tradeoff between local search for a solution and global response or proliferation of the solution. We demonstrate that the lymphatic network of the NIS efficiently balances local and global communication, and we suggest a new approach for Artificial Immune Systems (AIS) that uses a sub-modular architecture to facilitate distributed search.

**Keywords** Artificial immune system · Immune system scaling · Lymph node · West Nile Virus · Multi-robot control · Distributed search

S. Banerjee (✉) · M. Moses
Department of Computer Science, University of New Mexico, Albuquerque, NM 87131, USA
e-mail: soumya@cs.unm.edu

M. Moses
e-mail: melaniem@cs.unm.edu

## 1 Introduction

Many emerging pathogens infect multiple host species (Woolhouse et al. 2001), and multi-host pathogens may have very different dynamics in different host species (Cable et al. 2007). Understanding how quickly pathogens replicate and how quickly the natural immune system (NIS) responds is important for predicting the epidemic spread of emerging pathogens. We show that pathogen replication rates decline systematically with increasing host body size, but NIS response times do not increase significantly. We discuss how the decentralized architecture of the immune system facilitates parallel search, enabling NIS response times that do not increase substantially with body size.

The NIS solves a search problem in both physical space and antigen space. For the pathogens considered here, the length of the search is determined by the time it takes for a cognate B cell to encounter antigen. Encounter times depend on the size of the physical space in which the search occurs. This is a difficult search problem since very rare antigen-specific NIS cells have to search for small quantities of antigen throughout the body. For example, a mosquito injects $10^5$ live West Nile Virus particles into a vertebrate host that has billions or trillions of cells (Styer et al. 2007). The research we describe here suggests that the time for the immune system to detect and neutralize the pathogen is nearly independent of the size of the organism. We call this *scale-invariant detection and response*.

This is counter-intuitive, since if we inject a sparrow and a horse with the same amount of pathogen, the immune system of the horse has to search a much larger physical space to find the pathogen, compared to the sparrow. This research models how different potential architectures of the lymphatic network enable the NIS to mount an effective immune response that neutralizes pathogens in time that is independent of host body size. Physical space and resource limitations can also constrain Artificial Immune Systems (AIS). Our research shows how the optimal design of such AIS can be informed by architectural strategies employed by the NIS.

In addition to the immune system having to search larger spaces in larger organisms, larger body size may be expected to slow immune system response times because the metabolic rate of cells is lower in larger species (Brown et al. 2004). The metabolic rate of each cell is constrained by the rate at which nutrients and oxygen are supplied by the cardiovascular network. The rate at which this network supplies nutrients to each cell ($R_{\text{cell}}$) scales as the body mass ($M$) raised to an exponent of $-1/4$: $R_{\text{cell}} \propto M^{-1/4}$ such that individual cellular metabolic rates decrease as the body mass increases (West et al. 1997; Brown et al. 2004). The metabolic rate of a cell dictates the pace of many biological processes (Brown et al. 2004). This could affect NIS search times by reducing movement and proliferation of immune cells (Wiegel and Perelson 2004). Rates of DNA and protein synthesis are also dependent on the cellular metabolic rate and could influence the rate at which pathogens replicate inside infected cells (Cable et al. 2007).

The possibilities that NIS cells and pathogens may move and proliferate at speeds independent of mass ($\propto M^0$) or proportional to cellular metabolic rate ($\propto M^{-1/4}$) lead to four hypotheses, shown in Table 1, as originally proposed by Wiegel and Perelson (2004).

We combine an ordinary differential equation model, an Agent Based Model (ABM) and empirical results from experimental infection studies on West Nile Virus (WNV) (Komar et al. 2003; Bunning et al. 2002; Austgen et al. 2004) in what is the first test that we are aware of examining the effects of body size on pathogen replication and immune system response rates. Our results are consistent with H2: pathogen replication rate $\propto M^{-1/4}$ and NIS rates $\propto M^0$.

The remainder of the paper is organized as follows: Sect. 2 gives an introduction to the relevant immunology; our statistical methods are outlined in Sect. 3; Sect. 4 discusses an

**Table 1** Four scaling hypotheses of pathogen replication and immune system response rate (Wiegel and Perelson 2004)

| | |
|---|---|
| H1: Pathogen replication rate $\propto M^0$<br>NIS search rates $\propto M^0$ | H2: Pathogen replication rate $\propto M^{-1/4}$<br>NIS search rates $\propto M^0$ |
| H3: Pathogen replication rate $\propto M^0$<br>NIS search rates $\propto M^{-1/4}$ | H4: Pathogen replication rate $\propto M^{-1/4}$<br>NIS search rates $\propto M^{-1/4}$ |

ordinary differential equation model of pathogen growth and immune response; Sect. 5 discusses the difficulties faced by the NIS in searching space; we use an ABM to derive scaling relations for NIS cell detection and migration times in Sect. 6; the results are summarized in Sect. 7; Sect. 8 explains how a sub-modular NIS architecture balances fast search times and fast communication to recruit NIS cells, leading to scale-invariant detection; Sect. 9 discusses the applications and implications for this work in distributed AIS using an example of multi-robot control, and lastly we make concluding remarks in Sect. 10.

## 2 A Brief introduction to the immune system

The NIS has two main components: the innate immune system and the adaptive immune system. The innate immune system is the first line of defense of an organism and consists of complement proteins, macrophages and dendritic cells (DC) (Janeway et al. 2005). The adaptive immune system consists of T helper cells, B cells and cytotoxic T cells. The area of tissue that drains into a lymph node (LN) is called its draining region (DR). The lymphatic system collects extra-cellular fluid called lymph from tissues and returns it to blood (Janeway et al. 2005). DCs sample the tissue in DRs for pathogens, and upon encountering them, migrate to the nearest LN T cell area to present antigen to T helper cells. Cognate T helper cells specific to a particular pathogen are very rare (1 in $10^6$ NIS cells) (Soderberg et al. 2005). Upon recognizing cognate antigen on DCs, T helper cells proliferate and build up a clonal population in a process called clonal expansion. While proliferating, T helper cells also migrate to the LN B cell area to activate B cells. Cognate B cells specific to a particular pathogen are also very rare. They need to recognize cognate antigen on follicular dendritic cells and also need stimulation from cognate T helper cells. After recognition, cognate B cells undergo clonal expansion and differentiate into antibody-secreting plasma cells (Janeway et al. 2005).

This difficult search through the large physical space is facilitated by infected site inflammation, chemokines and preferential expression of adhesion molecules which guide NIS cells to sites of pathogen invasion (Janeway et al. 2005). The infected site LN recruits NIS cells from other LNs and blood through high endothelial venules. We refer to the recruitment time as communication overhead between LNs. Some pathogens do not invoke all the arms of the immune system, e.g. some bacteria are efficiently eliminated by the innate immune system. We focus here on pathogens, like WNV, that elicit an antibody response. However, the arguments put forward in this paper would apply also to other pathogens that spread systemically throughout the body and evoke a cytotoxic T cell or other response (see Sect. 8).

We are interested in the physical structure of the NIS, and we hypothesize that evolutionary pressures have shaped NIS architecture to minimize the time taken to unite rare antigen-specific NIS cells with their pathogens. This requires both rapid detection of the initial pathogens and also rapid clonal expansion to produce sufficient T helper cells to activate

a critical number of B cells. These B cells will then undergo clonal expansion and differentiate into antibody-secreting plasma cells. Hence this paper focuses primarily on the uptake of antigen by DCs in DR, recognition of antigen on DCs by T cells in LN, the subsequent process of clonal expansion and recruitment of B cells from other LNs.

## 3 Statistical methods

We use ordinary least squares (OLS) regression to test whether our model predictions are consistent with hypothesized scaling relationships and, where possible, biological measurements. We calculate the $r^2$ value, where $r$ is the Pearson correlation coefficient and the $r^2$ quantifies the proportion of variation that the independent variable explains in the dependent variable. We test how empirical data from literature and results of our simulation scale with mass by taking the logarithm of both variables and doing an OLS regression. We report whether the scaling exponent is consistent with $-0.25$, 0, or both. We test for significance at the alpha $= 0.05$ level. The mean is reported after testing all log-transformed datasets for normality using the Jarque–Bera test (Jarque and Bera 1987).

## 4 An ordinary differential equation model for viral dynamics

A standard Ordinary Differential Equation (ODE) model was developed to estimate how viral proliferation rates and immune response rates scale with body size, and model results were parameterized to match empirical levels of virus in blood (Banerjee and Moses 2009). Data on viral proliferation was taken from studies which used the same West Nile Virus strain to experimentally infect 25 different species with body mass ranging from 0.02 kg (house finch) to 390 kg (horse), and the viral load was monitored each day in blood serum (reported in plaque forming units—a measure of the number of infectious virions) over a span of 7 days post infection (d.p.i.) (Komar et al. 2003; Bunning et al. 2002; Austgen et al. 2004). In the model, $p =$ rate of virion production per infected cell, $\gamma =$ innate immune system mediated virion clearance rate, $\omega =$ adaptive immune system proliferation rate, and $t_{\mathrm{pv}} =$ time to attain peak viral concentration. Equations (1) to (4) are shown below:

$$\frac{dT}{dt} = -\beta T V \tag{1}$$

$$\frac{dI}{dt} = \beta T V - \delta I \tag{2}$$

$$\frac{dV}{dt} = pI - c(t)V \tag{3}$$

$$c(t) = \begin{cases} \gamma, & t < t_{\mathrm{pv}} \\ \gamma e^{\omega(t - t_{\mathrm{pv}})}, & t \geq t_{\mathrm{pv}} \end{cases} \tag{4}$$

Target cells $T$ are infected at a rate proportional to the product of their population size and the population size of virions $V$, with a constant of proportionality $\beta$. The loss in the target cell population is balanced by a gain in the infected cell population. Infected cells $I$ die at a rate $\delta I$. Virions are produced by infected cells at a rate $p$ and cleared by the immune system at the rate $c(t)V$. The action of the immune system is decomposed into an innate

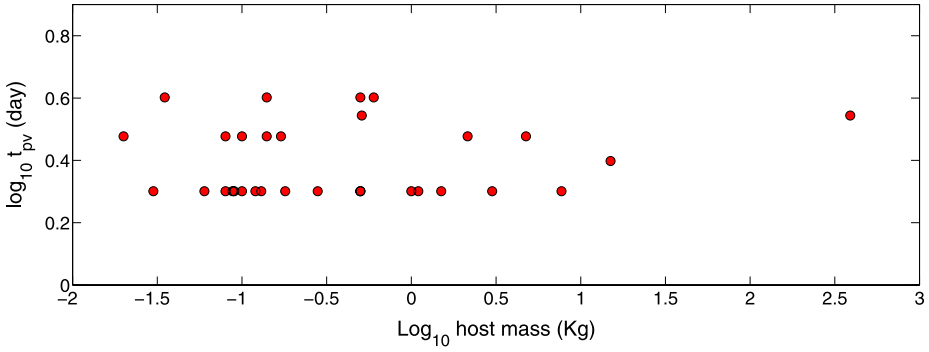


**Fig. 1** Plot of $\log_{10} t_{\text{pv}}$ (empirically measured time between infection and peak viral concentration in blood, units of day) vs. $\log_{10}$ host body mass $M$ (p-value testing significance of the slope = 0.35, 95% confidence interval on slope = $[-0.037, 0.0607]$, data from Komar et al. 2003; Bunning et al. 2002; Austgen et al. 2004)

response ($\gamma$) before the virus concentration attains a peak, and an exponential adaptive immune response after peak due to clonal expansion characterized by a proliferation rate $\omega$. This paper focuses on $p$ as pathogen replication, and $\gamma$ and $\omega$ as immune system response.

Empirical data show that time to peak viral concentration ($t_{\text{pv}}$, time between infection and peak viral concentration in blood) for WNV empirically occurs between 2–4 days post infection (Fig. 1) (Komar et al. 2003; Bunning et al. 2002; Austgen et al. 2004). If this peak were due to target cell limitation, then we would expect $t_{\text{pv}}$ to increase with host mass $M$ since larger animals have more target cells. However, $t_{\text{pv}}$ is likely to be determined by WNV-specific antibodies, which have a critical role in WNV clearance (Diamond et al. 2003). If the peak is determined by a threshold presence of antibodies, then it implies that $t_{\text{pv}}$ is determined by the time for cognate B cells to recognize antigen, proliferate and produce antibodies: $t_{\text{pv}} = t_{\text{detect}} + t_{\text{prolif}}$. Empirically, $t_{\text{pv}}$ is independent of host mass (Komar et al. 2003). The time $t_{\text{pv}}$ is highly conserved, ranging only between 2 and 4 days post infection across different hosts that range in mass from 0.02 kg (house finch) to 390 kg (horses). Since there is no statistically significant relationship between $t_{\text{pv}}$ and $M$ (Fig. 1) (p-value testing significance of the slope—0.35, 95% CI on slope—$[-0.037, 0.0607]$), then the data are consistent with the hypothesis that $t_{\text{pv}} \propto M^0$. Hence empirical data for WNV supports the hypothesis that NIS response rates are independent of $M$. One explanation that has been proposed is preferential metabolism, i.e. LNs are supplied energy at a rate which is independent of host body mass so that the metabolic rates of B cells and T cells in LN are independent of mass (Wiegel and Perelson 2004).

Other empirical data suggests that pathogen replication rates scale as $M^{-1/4}$ for a variety of pathogens in a variety of hosts, including WNV in birds and mammals (Cable et al. 2007). The Cable et al. study shows that times for a pathogen to cause symptoms or death is proportional to $M^{1/4}$ (where times are inverses of rates, mean exponent = 0.21, Table 1, Cable et al. 2007). Together, these observations reject all hypotheses in Table 1 except H2: pathogen replication declines with $M^{-1/4}$ and immune response times are invariant with respect to $M$. Ideally we would test all four hypotheses simultaneously using the ODE model described by (1) to (4). However, the ODE has too many parameters to simultaneously test both hypotheses without overfitting the data. Since our main goal is to determine the scaling of the NIS response rates and times, we fit the data by choosing initial parameter estimates consistent with pathogen replication rates scaling as $M^{-1/4}$, and then fit the model to the data.

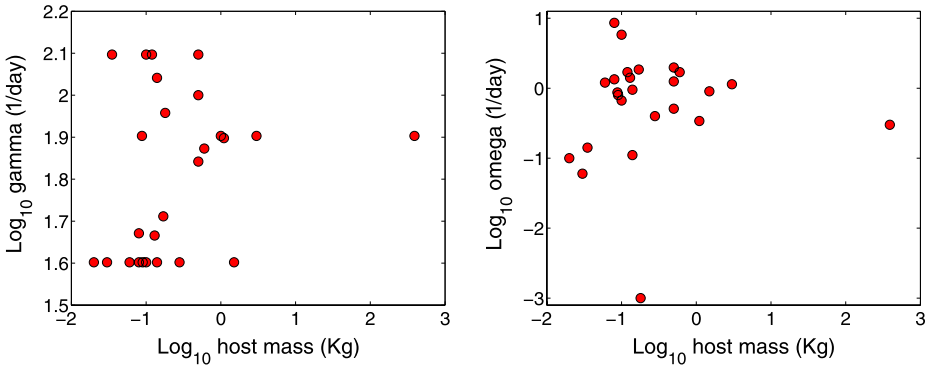


**Fig. 2** *Left panel*: plot of $\log_{10}\gamma$ (model estimated innate immune system mediated pathogen clearance rate, units of day$^{-1}$) vs. $\log_{10}$ host body mass $M$ (p-value testing significance of the slope $= 0.4238$, 95% confidence interval on slope $= [-0.04, 0.146]$). *Right panel*: plot of $\log_{10}\omega$ (model estimated adaptive immune system cell proliferation rate, units of day$^{-1}$) vs. $\log_{10}$ host body mass $M$ (p-value testing significance of the slope $= 0.7242$, 95% confidence interval on slope $= [-0.347, 0.4319]$)

The ODE model was fit to the viral load data for each of 25 species (Komar et al. 2003; Bunning et al. 2002; Austgen et al. 2004) for days 1–7 and the model parameters were estimated using non-linear least squares regression. The Berkeley Madonna® (Macey and Oster 2001) software package was used to generate the fits and we assigned the parameter value to the mass of the species to do an OLS regression. The scaling relations found were: $p \propto M^{-0.29}$ (the predicted exponent of $-0.25$ is in the 95% CI, $r^2 = 0.31$, p-value testing significance of slope $= 0.0038$). The innate immune system mediated pathogen clearance rate (measured day$^{-1}$, $\gamma$) and adaptive immune system cell proliferation rate (measured day$^{-1}$, $\omega$) were independent of host mass $M$ (Fig. 2) (p-values testing significance of the slope—0.4238 and 0.7242, respectively, 95% CI on slope—$[-0.04, 0.146]$ and $[-0.347, 0.4319]$ respectively). A sample parameter estimate and model prediction is shown in Table 2 and Fig. 3.

These findings from our ODE model and empirical data are consistent with hypothesis H2: pathogen replication rates decline in larger hosts, but immune response is independent of host mass (scale-invariant detection and response). This raises the question: what mechanisms make NIS rates independent of host body mass and metabolism? The problem of slower metabolism in larger hosts can be circumvented in immune response if LNs have preferential metabolism, i.e. they consume energy which is independent of host mass (Wiegel and Perelson 2004). However, even if immune system cells are not constrained by the lower mass specific metabolism in larger organisms, it remains to be explained how larger spaces can be searched in invariant time.

## 5 Searching for a needle in a haystack

The NIS is confronted with a very difficult search problem. Extremely rare B cells or T cells specific to a particular antigen (1 antigen-specific T cell in $10^6$ T cells) (Miller et al. 2004) search for initially rare antigen in localized tissue. A constant number of virions is injected into a host by a mosquito, regardless of host size, for WNV (Styer et al. 2007) and other pathogens spread by mosquito vectors. Our analysis of the ODE model and the empirical

**Table 2** Estimated ODE model parameters for great-horned owl (PFU: Plaque Forming Units)

| $V_0$ ($\frac{\text{PFU}}{\text{mL}}$) | $\beta$ ($\frac{1}{\frac{\text{PFU}}{\text{mL}}*\text{day}}$) | $p$ ($\frac{1}{\text{PFU}*\text{day}}$) | $\delta$ ($\frac{1}{\text{day}}$) | $\gamma$ ($\frac{1}{\text{day}}$) | $\omega$ ($\frac{1}{\text{day}}$) | $t_{\text{pv}}$ ($\frac{1}{\text{day}}$) |
|---|---|---|---|---|---|---|
| 2.95 | $10^{-7}$ | 524.97 | 1.19 | 91.99 | 2.7 | 3 |

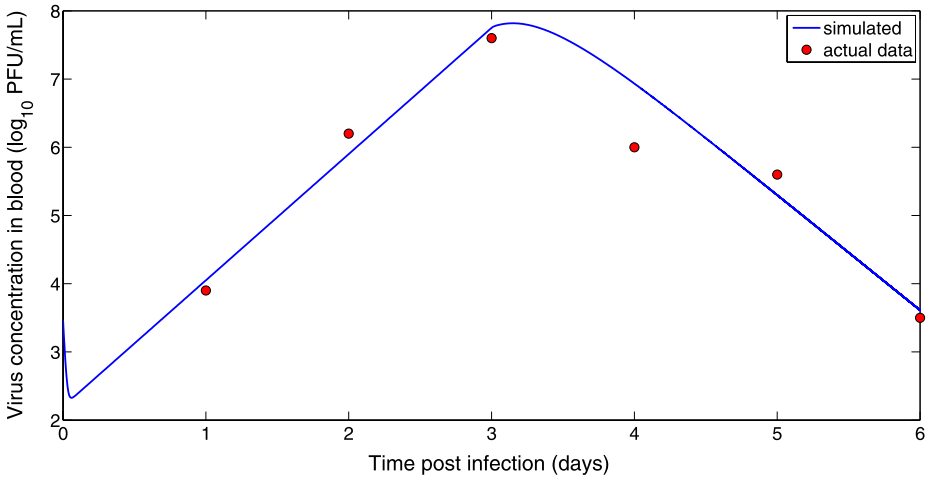


**Fig. 3** A sample plot of virus concentration in blood vs. time post infection (*solid line*—predicted ODE model output, *circles*—actual experimental data for a great-horned owl (data from Komar et al. 2003). *Y* axis—virus concentration in $\log_{10}$ PFU/mL of blood, *X* axis—days post infection

$t_{\text{pv}}$ suggest that the NIS in bigger organisms can find this fixed number of virus particles in approximately the same time as in smaller organisms, i.e. a horse finds those virions in a body (i.e. 'haystack') 10,000 times larger than a sparrow's body, but in the same time.

By way of introduction we define a completely modular system as one that is composed of self-contained units that are a fixed size and do not need to communicate, and a module as a LN and its DR. To simplify our models, we assume that each LN has a single DR and a DR drains into a single LN. Perfectly parallel search is easily achievable if an immune response is completely modular at the LN level and systemic communication in the immune system does not generate more overhead in larger systems. Completely modular systems have no overhead of communication and hence achieve perfectly parallel search (Amdahl 1967) since search is in a space of the same size and is replicated in parallel. However, experimental evidence suggests that the NIS is not modular at the LN level (see Sect. 8) (Halin et al. 2005; Altman and Dittmer 1974; Hildebrandt et al. 2005).

A conceptually similar concept of modularity has been proposed in protecton theory (Cohn and Langman 1990). A *protecton* is a modular unit of protection consisting of $10^7$ B cells of different specificities per mL of volume and is iterated proportionally to the size of the organism, i.e. if one samples 1 mL of a tadpole and 1 mL of an elephant, the same set of $10^7$ B cells will be found in each, but the elephant will have more copies of the protecton. This modular design reduces the time taken to build up a population of effector cells by clonal expansion. The protecton is a theoretical concept that the density and diversity of lymphocytes is constant across organisms. However, theory does not address how the lymphocytes constituting a protecton migrate through the body or how much communication

occurs between lymphocytes or LNs. This further motivates the question of investigating whether there is modularity at the level of LN that would help to parallelize the search process. Sections 6 and 7 explore the empirical architecture of LN organization, and explain why a purely modular architecture is not optimal.

## 6 Agent based model to explore how LN size affects NIS response time

The general model of immune system dynamics in the LN and its DR are shown in Fig. 4 and summarized as follows:

1. Stage 1: DCs randomly search for antigen in a local DR. The time taken to detect antigen is denoted by $t^{\mathrm{DC}}_{\mathrm{detect}}$.
2. Stage 2: DC migrates to a local LN T cell area along a chemotactic gradient. The time taken to migrate is $t^{\mathrm{DC}}_{\mathrm{migrate}}$.
3. Stage 3: Antigen-specific T cell in a LN detects antigen on DC and the time taken to detect is $t^{\mathrm{T\ cell,DC}}_{\mathrm{detect}}$. T cells then activate cognate B cells which undergo clonal expansion to produce antibody-secreting plasma cells.

Total time to detect antigen is given by

$$t_{\mathrm{detect}} = t^{\mathrm{DC}}_{\mathrm{detect}} + t^{\mathrm{DC}}_{\mathrm{migrate}} + t^{\mathrm{T\ cell,DC}}_{\mathrm{detect}} \tag{5}$$

We consider the time spent by the draining infected site LN in recruiting other NIS cells to it as the time spent in communication ($t_{\mathrm{comm}}$) (see Sect. 8).

We use an ABM to investigate how organization of the lymphatic network minimizes the time to detect antigen $t_{\mathrm{detect}}$ and $t_{\mathrm{comm}}$, leading to scale-invariant detection and response.

We note that the total volume of organs and fluids in mammals both scale proportional to $M$ (Peters 1983; West et al. 1997), so in our models, we assume that LN volume and the total volume of lymph in the entire body are both proportional to $M$. Thus, the number of LN multiplied by the volume of each LN is proportional to $M$. Additionally, the volume of a DR is determined by $M$ (which is proportional to body volume, given that tissue density is constant across animals) (Peters 1983) divided by the number of LN, i.e., for a fixed size $M$, more LN result in a smaller DR for each LN.

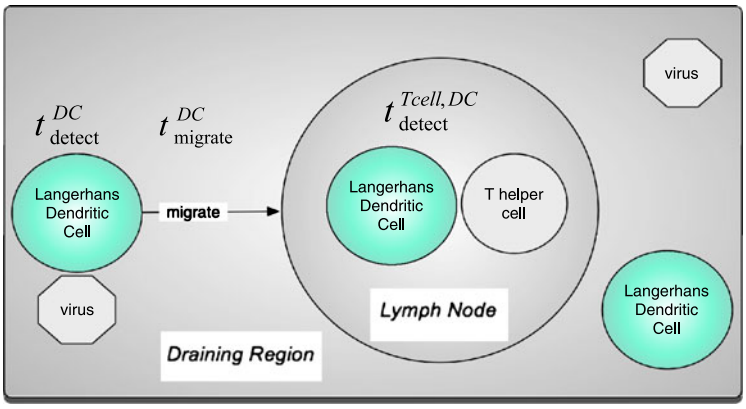


**Fig. 4** Immune system dynamics within a lymph node and its draining region

**Table 3** Parameters used in the Agent Based Model (L—literature, F—fit to data)

| Description | Value | Source |
|---|---|---|
| Side length of cubic compartment (DR) | 1000 μm to 4000 μm | L (Halin et al. 2005) |
| Side length of cubic compartment (LN) | 250 μm to 1000 μm | L (Halin et al. 2005) |
| Duration of a time step | 60 sec | F |
| Number of antigen-specific B cells in a lymph node of $10^6$ B cells | 1 | L (Miller et al. 2004) |
| Density of DC in DR | $1250/\text{mm}^3$ | L (Banchereau and Steinman 1998) |
| Amount of antigen in DR | 100 | L (Styer et al. 2007) |
| Radius of T cell | 10 μm | L (Miller et al. 2004) |
| Radius of antigen-presenting DC | 30 μm | L (Miller et al. 2004) |
| Speed of T cell | 0.1664 μm/sec | L (Miller et al. 2004) |
| Speed of antigen-presenting DC in LN | 0.0416 μm/sec | L (Miller et al. 2004) |
| Speed of antigen-presenting DC in DR | 0.0832 μm/sec | L (de Vries et al. 2003) |
| Sweep and sense distance of antigen-presenting DC (measured from cell center) | 50 μm | L (Miller et al. 2004) |

In order to explore how the spatial arrangement of LNs affects time to detect antigen, we use the CyCells (Warrender 2003, 2004) ABM to simulate viral replication in a 3D compartment representing the LN and DR. We simulated DCs, T cells, viruses and LNs, and explicitly modeled DC migration from tissue to LN along a chemotactic gradient, and random walk of DC and T cells in LN T cell area. The model parameters are summarized in Table 3.

The assumptions that we make are: (a) initially, we ignore migration of antigen-specific B cells from other LNs. We consider how such systemic responses change the NIS architecture in the next section; (b) there is a fixed chemotactic gradient for DCs to migrate into the LN; (c) for simplicity, we ignore pathogen replication in the tissue since WNV does not replicate until after it spreads to the LN and other organs; (d) DCs and T cells perform random walks in LN T cell area (Bajenoff et al. 2007); and (e) LNs have preferential metabolism (Wiegel and Perelson 2004), i.e. inside a LN, NIS cells have speed and proliferation rates that are invariant with host mass $M$.

## 7 Results

We first use an ABM to calculate the detection and migration times in (5) for mice and then show how each of these times scale with LN and DR dimensions. We then use these scaling relations to derive analytical expressions for detection, migration and communication times for three hypotheses of LN organization.

**Table 4** Simulated values in mice for DC antigen detection, DC migration and DC-T cell interaction

| Times | Dimensions (DR, LN) | Value (simulation) |
|---|---|---|
| $t^{\mathrm{DC}}_{\mathrm{detect}}$ | 4000 μm, 1000 μm | Mean = 26 minutes, SD = 32 minutes, 10 simulations |
| $t^{\mathrm{DC}}_{\mathrm{migrate}}$ | 4000 μm, 1000 μm | Mean = 3.7 hours, SD = 1.3 hours, 10 simulations |
| $t^{\mathrm{T\ cell,DC}}_{\mathrm{detect}}$ | 4000 μm, 1000 μm | Mean = 15.1 hours, SD = 6 hours, 10 simulations |

### 7.1 The base case model of a typical lymph node and scaling up

A DR was simulated as a cubic compartment of side 4000 μm with a cubic LN of length 1000 μm. The mean time taken by DCs to detect antigen and the time taken by an antigen-specific T cell to recognize antigen on DC are shown in Table 4 (due to the long execution time of the ABM, we took the average of 10 simulations). These are in agreement with experimental observations in mice (Miller et al. 2004). The total time to detect antigen ($t_{\mathrm{detect}} = t^{\mathrm{DC}}_{\mathrm{detect}} + t^{\mathrm{DC}}_{\mathrm{migrate}} + t^{\mathrm{T\ cell,DC}}_{\mathrm{detect}}$) is then around 19 hours. This is in agreement with experimental studies in mice (Itano and Jenkins 2003) and consistent with our observation that peak viral concentration occurs in day 2 to 4 for WNV across organisms, given our hypothesis that the peak occurs due to WNV-specific NIS cells, which must first have come into contact with WNV in the LN.

The DR and LN regions were then scaled up and we observed how DC detection, migration and T cell interaction times scaled with the size of the DR and LN. We simulated 3 cubic DRs: DR of length 1000 μm with LN of length 250 μm, DR of length 2000 μm with LN of length 500 μm, and DR of length 4000 μm with a LN of length 1000 μm. The observed scaling relations are in Table 5 and are consistent with DC migration time scaling linearly with the mean distance from DR to LN. The time for DC to detect antigen-specific T cell in LN was found to be uncorrelated with the size of the LN.

We now explore three competing hypotheses of lymphatic system organization (Fig. 5).

### 7.2 Model 1: Completely modular detection network

In our first model, we assume that the lymphatic network forms a *completely modular network* containing LN of constant size and number of LN proportional to organism size $M$. Using the scaling relationship for $t^{\mathrm{DC}}_{\mathrm{migrate}}$ from Table 5 and noting that in this model the LN and DR dimensions do not change with organism size gives us $t^{\mathrm{DC}}_{\mathrm{migrate}} \propto M^0$. Since the ABM predicts that detection times in LN do not depend on LN dimensions (Table 5) we have $t_{\mathrm{detect}} \propto M^0$ and hence the completely modular architecture gives us perfect scale-invariant detection. The predicted relations are summarized in Table 6.

### 7.3 Model 2: Non-modular detection network

The second model is the other extreme, that LNs are arranged in a detection network with a constant number of LN (all animals have the same number of LNs, however the size of LNs is larger in larger animals). In this model, the DR volume increases proportional to organism mass, and the average distance that a DC has to travel from the DR to the LN increases

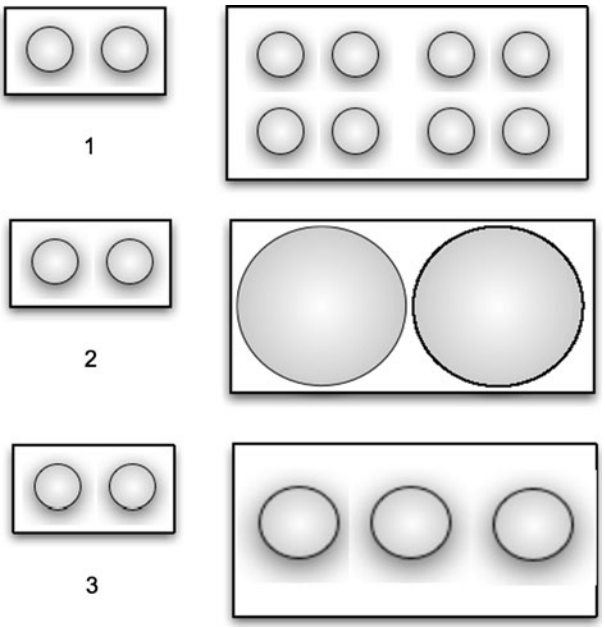


**Fig. 5** The 3 different hypotheses of scaling of lymph node size and numbers. (*1*) Completely Modular Detection Network: small animal with 2 LNs and another animal four times as big with four times the number of lymph nodes each of the same size as the small animal. (*2*) Non-Modular Detection Network: animal four times bigger has the same number of LNs but each is four times bigger. (*3*) Hybrid Sub-Modular Detection Network: animal four times bigger has more LNs each of which are also bigger

**Table 5** Scaling relations for time for DC antigen detection, DC migration and DC-T cell interaction ($l_{\mathrm{DR}}$ = length of DR compartment, $l_{\mathrm{LN}}$ = length of LN compartment). $^{+}$—testing for significance of exponent = 0

| Times | Dimensions (DR) | Scaling relation | Statistics |
|---|---|---|---|
| $t^{\mathrm{DC}}_{\mathrm{detect}}$ | 1000 μm, 2000 μm, 4000 μm | $\propto (l_{\mathrm{DR}} - l_{\mathrm{LN}})^0$ | p-value $= 0.18^{+}$ |
| $t^{\mathrm{DC}}_{\mathrm{migrate}}$ | 1000 μm, 2000 μm, 4000 μm | $\propto (l_{\mathrm{DR}} - l_{\mathrm{LN}})^1$ | $r^2 = 0.97$, $p < 0.001^{+}$ |
| $t^{\mathrm{T\ cell,DC}}_{\mathrm{detect}}$ | 1000 μm, 2000 μm, 4000 μm | $\propto l^0_{\mathrm{LN}}$ | p-value $= 0.23^{+}$ |

**Table 6** Scaling relations for LN and DR parameters and how $t^{\mathrm{DC}}_{\mathrm{migrate}}$ depends on DR and LN dimensions ($N$—number of LNs, $V_{\mathrm{lymph}}$—volume of lymph, $V_{\mathrm{LN}}$—volume of LN). $^{\S}$—taken from empirical data (Altman and Dittmer 1974)

| LN architecture | $N$ | $V_{\mathrm{lymph}} \propto N * V_{\mathrm{LN}}$ | $V_{\mathrm{LN}}$ | $V_{\mathrm{DR}} \propto M/N$ | $t^{\mathrm{DC}}_{\mathrm{migrate}} \propto (l_{\mathrm{DR}} - l_{\mathrm{LN}})$ | $t_{\mathrm{comm}} \propto M/V^2_{\mathrm{LN}}$ |
|---|---|---|---|---|---|---|
| Model 1 | $M^1$ | $M^1$ | $M^0$ | $M^0$ | $M^0$ | $M^1$ |
| Model 2 | $M^0$ | $M^1$ | $M^1$ | $M^1$ | $M^{1/3}$ | $M^{-2}$ |
| Model 3 | $M^{1/2\S}$ | $M^1$ | $M^{1/2}$ | $M^{1/2}$ | $M^{1/6}$ | $M^{-1/2}$ |

with organism mass as $M^{1/3}$ (Table 6). Hence $t^{\mathrm{DC}}_{\mathrm{migrate}} \propto M^{1/3}$. Since DC migration times are approximately 4 hours in mice, this model predicts that DC migration times in horses (which are 25,000 larger than mice) will be 30 times more than that in mice. This would necessitate migration times that are 5 days in horses and greater than the total observed time

for antibody response. Hence the hypothesis of complete lack of modularity in the NIS is inconsistent with observations.

### 7.4 Model 3: Hybrid sub-modular architecture

This architecture lies midway between Model 1 and Model 2. In this model LNs increase in both size and in numbers as animal size increases, and so does the size of the DR. Table 6 gives the predicted relation for $t^{\mathrm{DC}}_{\mathrm{migrate}} \propto M^{1/6}$. This will lead to migration times that are only five times longer in horses (around 20 hours) than in mice. It is not implausible that detection should take so long in a horse, and these slight increases in detection time might be compensated for by slower rates of exponential growth by the pathogen, as predicted by our ODE model (Sect. 4). Hence the sub-modular architecture produces detection times which are consistent with our empirical observations (scale-invariant detection), since the difference between 4 hours and 20 hours cannot be resolved on the basis of measurements of viral load taken every 24 hours.

## 8 Sub-modular architecture balances tradeoff between local and global communication

The limited published empirical data that we could find suggest that the mammalian NIS has a hybrid sub-modular architecture (Model 3). There is a trend of increasing LN size and number as animal size increases, for example, 20 g mice have 24 LN averaging 0.004 g each, and humans are 3000 times bigger and have 20 times more LN, each 200 times bigger (Halin et al. 2005; Altman and Dittmer 1974). Data from elephants (with LN approaching the size of an entire mouse) and horses (with 8000 LN) also support the hypothesis that LN size and number both increase with body size (Model 3) (Hildebrandt et al. 2005; Altman and Dittmer 1974); however, data for more species are required to statistically reject any of our 3 models.

We hypothesize that the NIS is sub-modular (consistent with Model 3) because it is selected not just to minimize time to detect pathogens (achieved by Model 1), but also to minimize the time to produce a sufficient concentration of antibody in the blood ($Ab_{\mathrm{crit}}$). A horse 25,000 times larger than a mouse must generate 25,000 more absolute quantities of antibody ($Ab$) in order to achieve the same concentration of antibody in the blood (where blood volume is $\propto M$) (Peters 1983). A fixed antibody concentration is required to fight infections like WNV that spread systemically through the blood. We can now consider that the NIS has evolved to minimize two quantities: the time to detect antigen ($t_{\mathrm{detect}}$), and the time ($t_{\mathrm{produce}}$) to produce $Ab$, where $Ab$ is proportional to $M$ ($Ab$ is the absolute quantity of antibody required to neutralize the pathogen in blood).

In all pathogens which evoke the adaptive immune system, the rate limiting step is the recognition of antigen on DCs by antigen-specific T helper cells within the LN T cell area (Soderberg et al. 2005). The time taken in this recognition step impacts other downstream processes like activation of B cells since T helper cells activated by DCs must migrate to the B cell area to activate B cells. If organisms of all body sizes activated the same number of initial B cells prior to clonal expansion, the time for a fixed number of B cells to produce $Ab$ would be $\propto \log_2 M$ (since B cells reproduce exponentially through clonal expansion). For example, since it takes 4 days of exponential growth of activated B cells to produce sufficient anti-WNV neutralizing antibody in mice (Diamond et al. 2003), then the corresponding time for a horse would be more than 2 months, should the same number of initial B cells be

activated prior to clonal expansion. This conflicts with empirical data on horses (Bunning et al. 2002). We assume that the NIS of larger organisms has to activate a larger number of initial B cells ($B_{\text{crit}}$) $\propto M$, in order to build up the critical density of antibodies in a fixed period of time. We now ask how the NIS can activate $B_{\text{crit}}$ in our three models.

In Model 1, LNs are a fixed size, and therefore contain a fixed number of B cells, and the smallest LNs (e.g. in mice) contain on the order of a single B cell that recognizes any particular pathogen. Thus, activating $B_{\text{crit}}$ to fight an infection like WNV that is initially localized in a single DR, requires recruiting B cells from distant LN. We consider this activation of B cells from remote LN as communication overhead. In general, the number of LNs that a single infected site LN has to communicate with ($N_{\text{comm}}$) in order to recruit more B cells is proportional to the amount of antibody required to neutralize the pathogen divided by the number of B cells resident in a LN ($Num_{\text{Bcell}}$): $N_{\text{comm}} \propto Ab/Num_{\text{Bcell}}$. Noting that $Ab \propto M$ and $Num_{\text{Bcell}} \propto V_{\text{LN}}$ we have $N_{\text{comm}} \propto M/V_{\text{LN}}$

The rate at which new B cells from other LN enter into an infected site LN through the blood or lymphatic vessels ($rate_{\text{comm}}$) is proportional to the volume of the LN, $rate_{\text{comm}} \propto V_{\text{LN}}$ (assuming that a larger LN will have proportionally higher number of endothelial venules and hence can recruit at a higher rate). The time spent in communicating with other LNs and recruiting and activating other B cells ($t_{\text{comm}}$) is then given by

$$t_{\text{comm}} = N_{\text{comm}}/rate_{\text{comm}} \propto M/V_{\text{LN}}^2 \tag{6}$$

Hence in Model 1, there are increasing costs to communicating with other LN as the organism gets bigger ($t_{\text{comm}} \propto M$); it carries out efficient search but is not optimized for antibody production.

Model 2 (non-modular detection network) compensates for the limitation of physically transporting NIS cells over larger distances by making LNs bigger in larger organisms ($V_{\text{LN}} \propto M$). This increases the rate of influx of B cells ($rate_{\text{comm}} \propto V_{\text{LN}} \propto M$) and also situates more NIS cells inside the infected site LN. Since all the necessary NIS cells that need to be activated are within the LN, this architecture has no communication cost. However, as shown above (Sect. 7.3), Model 2 leads to DC migration times that are prohibitively long for large animals ($t_{\text{migrate}}^{\text{DC}} \propto M^{1/3}$).

The architecture that strikes a balance between the two opposing goals of antigen detection (local communication) and antibody production (global communication) is Model 3 (hybrid sub-modular architecture). It minimizes $T = t_{\text{detect}} + t_{\text{produce}}$, where $t_{\text{detect}}$ = time taken to detect antigen, and $t_{\text{produce}}$ = time taken to produce antibody = $t_{\text{comm}}$ (since the time taken to produce antibodies is equal to the time taken to recruit B cells or communicate with other LNs; after recruitment starts and cognate T cells recognize antigen on DCs, T cells can migrate to the B cell area and activate B cells in parallel to the recruitment process described earlier).

We can solve for the total time ($T = t_{\text{detect}} + t_{\text{produce}}$) to detect antigen and produce B cells using (7) and the scaling relationship for $t_{\text{migrate}}^{\text{DC}}$ from Table 5 giving:

$$T = t_{\text{detect}}^{\text{DC}} + a(l_{\text{DR}} - l_{\text{LN}}) + t_{\text{detect}}^{\text{T cell,DC}} + bM/V_{\text{LN}}^2 \tag{7}$$

where $a$ and $b$ are constants, $l_{\text{DR}}$ = length of DR, $l_{\text{LN}}$ = length of LN, $V_{\text{LN}}$ = volume of LN, $M$ = organism mass, and $N$ = number of LNs. This becomes

$$T = t_{\text{detect}}^{\text{DC}} + cV_{\text{LN}}^{1/3} + t_{\text{detect}}^{\text{T cell,DC}} + bM/V_{\text{LN}}^2 \tag{8}$$

where $c$ is a constant, and $l_{\text{DR}}$ and $l_{\text{LN}}$ scale as $V_{\text{DR}}^{1/3}$ and $V_{\text{LN}}^{1/3}$ respectively. Since $V_{\text{LN}}$ and $V_{\text{DR}}$ scale isometrically (as $M/N$), then $l_{\text{DR}} - l_{\text{LN}} \sim V_{\text{LN}}^{1/3}$.

Differentiating with respect to $V_{LN}$ and setting the derivative to zero to find the minimum $T$, gives

$$V_{LN} \propto M^{3/7} \tag{9}$$

Since the amount of lymph is proportional to host body mass ($N * V_{LN} \propto M$), then

$$N \propto M^{4/7} \tag{10}$$

These predictions are consistent with the few empirical data we were able to obtain. Similar arguments would also apply to other pathogens that spread systemically throughout the body and need to activate a number of B cells or cytotoxic T cells proportional to $M$. We note that Perelson and Wiegel (2009) predict that $N \propto M^{1/2}$, but that analysis did not explicitly consider an optimization to simultaneously minimize detection time and time to produce the critical number of $Ab$.

In summary, due to the requirement of activating increasing number of NIS cells for antibody production in larger organisms, there are increasing costs to global communication as organisms grow bigger. The semi-modular architecture (Model 3) balances the opposing goals of detecting antigen using local communication and producing antibody using global communication between LNs. This leads to optimal antigen detection and antibody production time, and nearly scale-invariant detection and response.

## 9 Relevance to artificial immune systems

The natural immune system utilizes an architecture that functions within constraints imposed by physical space. Physical space is also an important constraint on artificial immune systems, especially in applications used to connect inexpensive low-powered sensors using short-range wireless communication (Kleinberg 2007). Such spatial networks are being increasingly used in environmental monitoring, disaster relief and military operations (Kleinberg 2007). These networks might operate under constraints of resource and physical space, similar to an NIS. Although there are systematic differences between an NIS and an AIS (Timmis et al. 2008), the design of the AIS can be informed by architectural strategies employed by their biological counterpart.

### 9.1 Original system

As a concrete example of an application where space is a constraint and scaling of performance with system size is an important design criterion, we consider an AIS approach to control multiple robots tasked with obstacle avoidance (Nair and Godfrey 2008). The robots communicate with software agent(s) in a server upon encountering an obstacle. The agents transmit rule-sets of actions to robots to help overcome their obstacles, and agents also share information globally amongst themselves by migrating to other computer servers. Some analogies between this AIS and an NIS are: the obstacle problem presented by a robot is analogous to an antigen, the rule-set of actions transmitted by an agent correspond to antibodies, the robots are akin to DCs, software agents correspond to B cells, the computer servers themselves are analogous to LNs, and the physical area ‘serviced’ by a single computer server corresponds to a DR. The system is diagrammed in Fig. 6 (modified from Nair and Godfrey 2008).

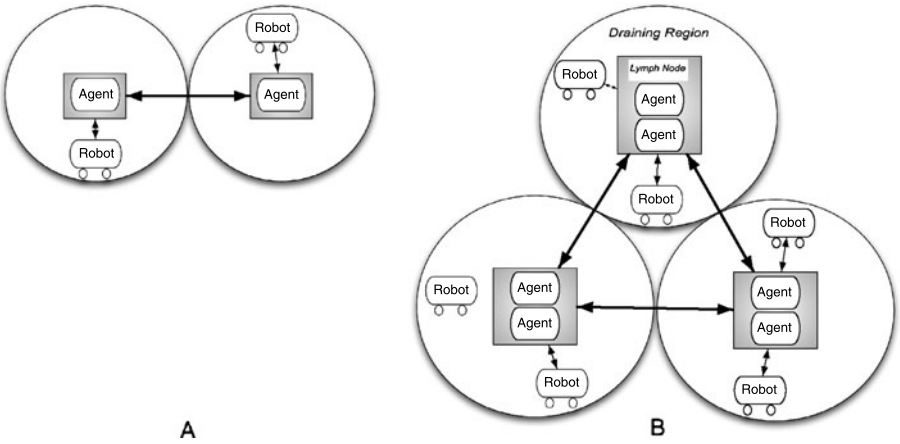


**Fig. 6** (**A**) *Left panel*: a scaled down version of the multi-robot AIS system. The shaded regions are artificial LNs (computer servers) and the unshaded regions are the artificial DR. Light arrows denote communication between robots and servers (local communication) and bold arrows denote communication between servers (global communication). (**B**) *Right panel*: a scaled up multi-robot AIS system with sub-modular architecture. Note that the number of artificial LNs and their size (the number of robots they service and the number of software agents they have in memory) both increase with the size of the system

### 9.2 Modifying the original system using a sub-modular architecture

We are interested in an architecture that minimizes the time taken by a robot to transmit information about an obstacle (local detection), the time taken by a computer server to transmit back an initial rule-set of actions (local response) and the time taken by a computer server to communicate good rule-sets to other agents (global response). There are two potential communication bottlenecks: communication between robots and computer servers, and communication between computer servers.

Overcoming the bottleneck in (local) communication between robot and server requires many small DRs. A bottleneck in (global) server communication requires a few large servers. If both local and global communication are constrained, the architecture which balances these opposing requirements is sub-modular, i.e. the number of servers increases sublinearly with system size and the capacity of each server (bandwidth, memory and number of robots serviced by each server) increases sublinearly with system size (shown in Fig. 6). The four ways in which communication can be bottlenecked are outlined below:

1. High Capacity Robot Bandwidth, High Capacity Server Bandwidth: Assuming that robots have high bandwidth to communicate with computer servers and software agents can communicate with each other over a channel with high bandwidth, we see that trivially any of the architectures would suffice.
2. Limited Robot Bandwidth, High Capacity Server Bandwidth: Assuming communication between robots and computer servers is a bottleneck mandates a small fixed size DR, i.e. a computer server servicing a small number of robots to reduce contention and transmission time. Since communication between servers is not constrained, we can have the number of servers scaling linearly with system size, giving Model 1 (completely modular network) as the optimal architecture.
3. High Capacity Robot Bandwidth, Limited Server Bandwidth: Assuming communication between computer servers is a bottleneck stipulates a fixed number of computer servers

to reduce communication overhead. Since communication between robots and servers is not constrained, we can have the DR size (number of robots serviced by a single server) and LN size (number of agents in a single server) scaling with system size. Hence the optimal architecture is Model 2 (non-modular detection network).

4. Limited Robot Bandwidth, Limited Server Bandwidth: A bottleneck in robot and server communication demands a small DR and lots of servers, whereas a bottleneck in server communication requires fewer large servers. The architecture that balances these opposing requirements is Model 3 (hybrid sub-modular architecture), i.e. the number of servers and their size (number of robots serviced by each server) increases with system size (6).

The local communication time within an artificial DR is a function of the number of robots ($d$) serviced by a single artificial LN

$$t_{\text{local}} = f(d) \tag{11}$$

The function $f$ will depend on constraints on communication between robots and servers, influenced, for example, by how robot requests are queued on the server and the distance over which low power robots can send and receive messages. The global communication time between artificial LNs is also a function of the number of LNs in the system ($n/d$) where $n$ is the total number of robots in the entire system

$$t_{\text{global}} = g(n/d) \tag{12}$$

The function $g$ depends on communication constraints between servers. For low latency and high bandwidth connections among servers, $t_{\text{global}}$ may not scale appreciably. However, low power servers distributed in remote environments, may preclude broadcast communication such that $t_{\text{global}}$ increases with $n/d$. An increase in the size of an artificial LN (and hence the number of robots serviced, $d$) would reduce $t_{\text{global}}$ at the cost of $t_{\text{local}}$. The size and number of artificial LNs to balance local and global communication depends on the precise functions $f$ and $g$ mediating local and global communication.

Although we have provided only one example, this research is widely applicable to other distributed systems AIS applications. In recent work, we have extended our work to modify peer-to-peer systems with a sub-modular architecture (Banerjee and Moses 2010).

In summary, understanding the tradeoff between fast search for pathogens and fast production of antibodies is important for AIS that mimic the NIS. If the goal of an AIS is only search or detection in physical space with a local response, then a completely modular design (Model 1) will be optimal. If an AIS searches in physical space but requires a global response after detection, a sub-modular architecture (Model 3) optimizes the tradeoff between local search and global response and will lead to faster search and response times ($T = t_{\text{local}} + t_{\text{global}}$). Our analysis sheds light on the relationship between physical space and architecture in resource-constrained distributed systems.

## 10 Conclusions

Host body size constrains pathogen replication rates due to the physical characteristics of transportation networks that supply infected and normal cells with energy. Host body size also constrains NIS detection and response times by increasing the physical size of search spaces. The NIS is comprised of rare antigen-specific immune system cells that it must utilize to search for initially small numbers of pathogens localized in a large physical space.

The NIS solves this classic search for a 'needle in a haystack' in time that is almost invariant of the size of the organism. The decentralized nature of the lymphatic network also helps in efficient pathogen detection by acting as a small volume of tissue where DCs can efficiently present antigen to T cells. The NIS must also respond to the antigen by producing antibodies (in the case of WNV) proportional to the mass of the organism. From empirical data, that time also appears independent of body size.

We use an ODE model to show that NIS response rates are independent of host body size and pathogen replication rates decrease with body size. We examine three different hypothesized NIS architectures using an agent based model, to explain the scale-invariant detection and response times of the NIS. The sub-modular detection network strikes a balance between the two opposing goals of antigen detection (local communication) and antibody production (global communication), and is consistent with observed numbers and sizes of LN. This sub-modular architecture of the lymphatic network must simultaneously provide systemic protection to the entire body while protecting each local volume of tissue equally well. Thus, the lymphatic architecture lies between the extremes of the fully centralized cardiovascular network (in which blood is oxygenated in a single location) and the fully decentralized concept of the protecton (in which a fixed number and diversity of lymphocytes protects every volume of tissue).

We demonstrated that a sub-modular architecture effectively balances the tradeoff between local search for a solution and global distribution of the solution in distributed robot control. In addition to incorporating NIS inspired distributed search algorithms into AIS, we suggest that AIS can replicate the sub-modular architecture used by the NIS to balance the tradeoff between local and global communication.

**Acknowledgements** We acknowledge fruitful discussions with Dr. Alan Perelson, Dr. Stephanie Forrest, Dr. Jedidiah Crandall and Kimberly Kanigel, helpful reviews from the ICARIS 2009 conference and four anonymous referees for their insightful comments. We are also grateful to Dr. Nicholas Komar for sharing his experimental data with us. MEM and SB were supported by a grant from the National Institute of Health (NIH RR018754) to the University of New Mexico Center for Evolutionary and Theoretical Immunology. SB would also like to acknowledge travel grants from RPT, SCAP and PIBBS at the University of New Mexico.

## References

Altman, P., & Dittmer, D. (1974). *Biology data book*. Bethesda: Federation of American Societies for Experimental Biology.

Amdahl, G. (1967). Validity of the single processor approach to achieving large-scale computing capabilities. In *AFIPS '67 (Spring): Proceedings of the April 18–20, 1967, Spring joint computer conference* (pp. 483–485). New York: ACM.

Austgen, L., Bowen, R., Bunning, M., Davis, B., Mitchell, C., & Chang, G. (2004). Experimental infection of cats and dogs with West Nile Virus. *Emerging Infectious Diseases*, *10*(1), 82–86.

Bajenoff, M., Egen, J., Qi, H., Huang, A., Castellino, F., & Germain, R. (2007). Highways, byways and breadcrumbs: Directing lymphocyte traffic in the lymph node. *Trends in Immunology*, *28*(8), 346–352.

Banchereau, J., & Steinman, R. (1998). Dendritic cells and the control of immunity. *Nature*, *392*(6673), 245–252.

Banerjee, S., & Moses, M. (2009). A hybrid agent based and differential equation model of body size effects on pathogen replication and immune system response. In P. S. Andrews et al. (Eds.), *Lecture notes in computer science: Vol. 5666. Artificial immune systems, 8th international conference, ICARIS 2009* (pp. 14–18). Berlin: Springer.

Banerjee, S., & Moses, M. (2010). Modular RADAR: An immune system inspired search and response strategy for distributed systems. In E. Hart et al. (Eds.), *Lecture notes in computer science: Vol. 6209. Artificial immune systems, 9th international conference, ICARIS 2010* (pp. 116–129). Berlin: Springer.

Brown, J. H., Gillooly, J. F., Allen, A. P., Savage, V.M., & West, G.B. (2004). Toward a metabolic theory of ecology. *Ecology*, *85*(7), 1771–1789.

Bunning, M., Bowen, R., Cropp, C., Sullivan, K., Davis, B., Komar, N., Godsey, M., Baker, D., Hettler, D., Holmes, D., Biggerstaff, B., & Mitchell, C. (2002). Experimental infection of horses with West Nile Virus. *Emerging Infectious Diseases*, *8*(4), 380–386.

Cable, J., Enquist, B., & Moses, M. (2007). The allometry of host-pathogen interactions. *PLoS ONE*, *2*(11). doi:10.1371/journal.pone.0001130.

Cohn, M., & Langman, R. (1990). The Protecton: the evolutionarily selected unit of humoral immunity. *Immunological Reviews*, *115*, 9–147.

de Vries, I. J. M., Krooshoop, D. J. E. B., Scharenborg, N. M., Lesterhuis, W. J., Diepstra, J. H. S., van Muijen, G. N. P., Strijk, S. P., Ruers, T. J., Boerman, O. C., & Oyen, W. J. G. (2003). Effective migration of antigen-pulsed dendritic cells to lymph nodes in melanoma patients is determined by their maturation state. *Cancer Research*, *63*(12), 12–17.

Diamond, M., Sitati, E., Friend, L., Higgs, S., Shrestha, B., & Engle, M. (2003). A critical role for induced IgM in the protection against West Nile Virus infection. *Journal of Experimental Medicine*, *198*(12), 1853–1862.

Halin, C., Rodrigo Mora, J., Sumen, C., & von Andrian, U. H. (2005). In vivo imaging of lymphocyte trafficking. *Annual Review of Cell and Developmental Biology*, *21*, 581–603.

Hildebrandt, T., Hermes, R., Ratanakorn, P., Rietschel, W., Fickel, J., Frey, R., Wibbelt, G., Reid, C., & Goritz, F. (2005). Ultrasonographic assessment and ultra-sound guided biopsy of the retropharyngeal lymph nodes in Asian elephants (Elephas maximus). *Veterinary Record*, *157*(18), 544–548.

Itano, A., & Jenkins, M. (2003). Antigen presentation to nave CD4 T cells in the lymph node. *Nature Immunology*, *4*, 733–739.

Janeway, C., Travers, P., Walport, M., & Shlomchik, M. (2005). *Immunobiology: The immune system in health and disease*. New York: Garland Science.

Jarque, C., & Bera, A. (1987). A test for normality of observations and regression residuals. *International Statistical Review*, *55*(2), 163–172.

Kleinberg, J. (2007). Computing: The wireless epidemic. *Nature*, *449*, 287–288.

Komar, N., Langevin, S., Hinten, S., Nemeth, N., Edwards, E., Hettler, D., Davis, B., Bowen, R., & Bunning, M. (2003). Experimental infection of North American birds with the New York 1999 strain of West Nile Virus. *Emerging Infectious Diseases*, *9*(3), 311–322.

Macey, R. I., & Oster, G. (2001). *Berkeley Madonna, version 8.0*. Tech. rep., University of California, Berkeley, California.

Miller, M., Hejazi, A., Wei, S., Cahalan, M., & Parker, I. (2004). T cell repertoire scanning is promoted by dynamic dendritic cell behavior and random T cell motility in the lymph node. *Proceedings of the National Academy of Sciences*, *101*(4), 998–1003.

Nair, S., & Godfrey, W. (2008). An immune system based multi-robot mobile agent network. In P. J. Bentley et al. (Eds.), *Lecture notes in computer science: Vol. 5132*. *Artificial immune systems, 7th international conference, ICARIS 2008* (pp. 424–433). Berlin: Springer.

Perelson, A., & Wiegel, F. (2009). Scaling aspects of lymphocyte trafficking. *Journal of Theoretical Biology*, *257*(1), 9–16.

Peters, R. (1983). *The ecological implications of body size*. Cambridge: Cambridge University Press.

Soderberg, A., Payne, G., Sato, A., Medzhitov, R., Segal, S., & Iwasaki, A. (2005). Innate control of adaptive immunity via remodeling of lymph node feed arteriole. *Proceedings of the National Academy of Sciences*, *102*(45), 16,315–16,320.

Styer, L., Kent, K., Albright, R., Bennett, C., Kramer, L., & Bernard, K. (2007). Mosquitoes inoculate high doses of West Nile virus as they probe and feed on live hosts. *PLoS Pathogens*, *3*(9). doi:10.1371/journal.ppat.00310132.

Timmis, J., Hart, E., Hone, A., Neal, M., Robins, A., Stepney, S., & Tyrrell, A. (2008). *Immuno-engineering* (Vol. *268*). Berlin: Springer.

Warrender, C. (2003). CyCells (Open source software). URL http://sourceforge.net/projects/cycells.

Warrender, C. (2004). Modeling intercellular interactions in the peripheral immune system. Ph.D. thesis, University of New Mexico.

West, G., Brown, J., & Enquist, B. (1997). A general model for the origin of allometric scaling laws in biology. *Science*, *276*(5309), 122–126.

Wiegel, F. W., & Perelson, A. (2004). Some scaling principles for the immune system. *Immunology and Cell Biology*, *82*, 127–131.

Woolhouse, M., Taylor, L., & Haydon, D. (2001). Population biology of multihost pathogens. *Science*, *292*, 1109–1112.